

The Role of Primordial Kicks on Black Hole Merger Rates

Miroslav Micic^{1*}, Tom Abel² & Steinn Sigurdsson¹

¹ *Department of Astronomy & Astrophysics, Pennsylvania State University*

² *Department of Physics, Stanford University*

5 December 2018

ABSTRACT

Primordial stars are likely to be very massive $\geq 30 M_{\odot}$, form in isolation, and will likely leave black holes as remnants in the centers of their host dark matter halos in the mass range $10^6 - 10^{10} M_{\odot}$. Such early black holes, at redshifts $z \gtrsim 10$, could be the seed black holes for the many supermassive black holes found in galaxies in the local universe. If they exist, their mergers with nearby supermassive black holes may be a prime signal for long wavelength gravitational wave detectors. We simulate formation of black holes in the center of high redshift dark matter halos and explore implications of initial natal kick velocities conjectured by some formation models. The central concentration of early black holes in present day galaxies is reduced if they are born even with moderate kicks of tens of km/s. The modest kicks allow the black holes to leave their parent halo, which consequently leads to dynamical friction being less effective on the lower mass black holes as compared to those still embedded in their parent halos. Therefore, merger rates may be reduced by more than an order of magnitude. Using analytical and illustrative cosmological N-body simulations we quantify the role of natal kicks of black holes formed from massive metal free stars on their merger rates with supermassive black holes in present day galaxies. Our results also apply to black holes ejected by the gravitational slingshot mechanism.

Key words: IMBH, SMBH, Pop III, gravitational radiation, LISA, BBO

1 MOTIVATION

It is firmly established that most galaxies have super-massive black holes (SMBH) at their centers. Their masses are in the range $10^6 M_{\odot} \lesssim M \lesssim 10^9 M_{\odot}$ and it appears that there is a number of correlations (Kormendy & Gebhardt 2001, Gerhard 2001) between their masses and properties of the galactic bulge hosting them: mass of the SMBH on one hand and mass (Laor 2001) or luminosity or velocity dispersion (Merritt & Ferrarese 2001, Tremaine et al. 2002, Gebhardt et al. 2001) or light profile (Graham et al. 2001) of the galactic bulge on the other. These correlations point to the link between the formation of SMBHs and the evolution of their hosts. It also appears that SMBHs are linked to the properties of the host dark matter halos. If the SMBH precursors have been present from very early on, then their mergers, together with growth by accretion, could account for the abundance of the SMBHs today (Schneider et al. 2002).

Ab initio numerical simulations of the formation of the first luminous objects in the current structure formation models find metal free stars to form in isolation and may have masses $30 M_{\odot} \leq m \leq 300 M_{\odot}$ (Abel et al. 2000, Abel et al. 2002, Bromm et al. 2002). In current models of structure formation, dark matter initially dominates and pregalactic objects form because of gravitational instability from small initial density perturbations. As they assemble via hierarchical merging, the metal-free primordial gas cools through rotational lines of hydrogen molecules. In the absence of metals, H_2 is the main coolant below $\sim 10^4 K$, which is the temperature range typically encountered in collapsing Population III objects. Rotational transitions of H_2 , occurring via electric quadrupole radiation, allow the gas to cool and sink to the center of the dark matter

* E-mail: micic@astro.psu.edu, tabel@slac.stanford.edu, steinn@astro.psu.edu

potential well. This leads to a top-heavy initial stellar mass function and to the production of very massive stars, unlike the modern stellar IMF which is declining rapidly with increasing mass.

Metal-free, high mass Population III stars die after 3 Myr, losing only a small fraction of their mass. If the fragmentation occurs during core collapse, two or more compact objects (black hole or neutron star) could be produced. This suggests that a large population of primordial massive black holes (MBH from now, with mass $\leq 10^3 M_\odot$) could be an end product of such pregalactic star formation (Heger et al. 2003). Since they form in rare high- σ density peaks (Couchman & Rees 1986, Madau & Rees 2001), relic MBHs would be predicted to cluster in the cores of more massive halos (Abel et al. 2002) formed by subsequent mergers. It has been suggested (Volonteri et al. 2003, Islam et al. 2003) that mergers of massive halos and clustering of these MBHs should start at redshifts as large as $z \sim 20$. Growth of MBHs would proceed through accretion and coalescence which would lead to the formation of intermediate mass black holes (IMBH from now, with mass in range $10^3 M_\odot \leq m \leq 10^6 M_\odot$). IMBHs can form sufficiently early on. In the most optimistic scenario (Haiman & Loeb 2001), $10^9 M_\odot$ black hole could form at redshift $z \sim 10$. However, through the mergers of dark matter halos at high redshift, black holes would form binaries and their coalescence under gravitational radiation would give them a significant kick velocity (Favata et al. 2004, Merritt et al. 2004). Anisotropic emission of gravitational waves which carry away linear momentum causes center of mass recoil. The recoil velocities are expected to be most likely in the range $10\text{-}100 \text{ km s}^{-1}$, kicks of a few hundred km s^{-1} are not unexpected, and the largest recoils should not be above 500 km s^{-1} (Favata et al. 2004). The amplitude of the kick determines if the black hole will be ejected from its host dark matter halo or if it will fall back. Even the most massive dark matter halo at redshift $z \geq 11$ can not retain the black hole that received 150 km s^{-1} kick while at the redshift of $z \geq 8$, kicks of 300 km s^{-1} are sufficient to produce the same result (Merritt et al. 2004, Fig 3.). This is valid for black holes with masses $10^3 M_\odot \leq m \leq 10^8 M_\odot$. Fully general relativistic simulations of radiation recoil from highly distorted Schwarzschild holes yield maximum kick velocities in excess of 400 km/s (Brandt & Anninos 1999). This should be sufficient to: eject IMBHs from globular clusters; displace IMBHs from the centers of dwarf galaxies; perhaps provide sufficient population of IMBHs for merging at the centers of spiral galaxies (Merritt et al. 2004). In fact, for Kerr black holes, recoil is significant even for holes of equal mass (Favata et al. 2004) and may be directed out of the plane of the orbit (Redmount & Rees 1989). Kicks are also expected from the gravitational slingshot - the ejection of one or more black holes when three black holes interact (Xu et al. 1994, Valtonen et al. 2000, Rees 1988). Space velocities much greater than those of their progenitors are common in neutron stars (Lai et al. 2001, Colpi & Wasserman 2002, Arzoumanian et al. 1997). Recent studies of pulsar proper motion implies characteristic velocities of the order of $200\text{-}500 \text{ km s}^{-1}$ (Wex et al. 2000), and as large as 100 km s^{-1} for black holes (Colpi & Wasserman 2002). The high space velocity of X-ray Nova Sco 1994 implicates black hole kicks (Brandt et al. 1995). Likely values of the velocity of the merged objects at infinity lie in the range of $100 - 300 \text{ km s}^{-1}$ (Davies et al. 2002).

Without exploring the nature of kicks, we are investigating the observational implications of other peoples conjectures on black holes getting impulsive kicks, whether on formation or through mergers. We are also exploring the consequences that kicks will have on the IMBHs merger rates and the formation of SMBHs that are indirectly observed in the nuclei of nearby luminous galaxies. LISA will test the Population III IMBHs formation models.

A powerful instrument for studying IMBHs will be LISA (Danzmann 2003). LISA can study much of the last year of inspiral, as well as the waves from the final collision and coalescence of IMBHs binaries, whenever the masses of the black holes are in the range $3 \times 10^4 M_\odot \leq M \leq 10^8 M_\odot$. It can also study the final coalescences with remarkable signal to noise ratios: $S/N \geq 1000$. For black holes with the masses in the range $100 M_\odot \leq M \leq 10^4 M_\odot$, out to cosmological distances, LISA can observe the last few years of inspiral, but not the final collisions. The equal-mass black hole binaries enter LISA's frequency band roughly 1000 years before their final coalescences, more or less independently of their masses, for the range $100 M_\odot \leq M \leq 10^6 M_\odot$. If the coalescence rate is one per year, LISA would see roughly 1000 additional IMBHs binaries that are slowly spiraling inward, with measurable inspiral rates. From the inspiral rates, the amplitudes of the two polarizations, and the waves' harmonic content, LISA can determine each such binary's luminosity distance, redshifted chirp mass $(1+z)M_c$, orbital inclination, and eccentricity. From the waves' modulation by LISA's orbital motion, LISA can learn the direction to the binary with an accuracy of order one degree (Thorne 1995, Cornish & Levin 2002, Vecchio et al. 2004).

In addition to the mapping of spacetime around SMBH with inspiraling compact objects, BBO (Big Bang Observer) mission will have arcsecond-arcminute precision in identifying and localizing every merging black hole binary at any redshift, anywhere in the universe over the years to months before their actual merger. In combination with ground-based detectors at higher frequencies, it will measure the mass, angular momenta, and dynamic spacetime structure of these compact objects with unprecedented precision.

If these IMBHs would accrete from the interstellar medium they may also be found by deep X-ray observations (Agol & Kamionkowski 2002) in the Milky Way. This observational signature will depend sensitively on the spatial distribution of these black holes in our galaxy. Similarly, the next generation of micro-lensing searches may be able to constrain high mass black holes from the longest events (Agol et al. 2002).

In our numerical simulations we use GADGET (GALaxies with Dark matter and Gas intErAcT), a code written by Volker Springel (Springel et al. 2001), for simulations of self-gravitating collisionless fluids evolution, with a tree method N-body approach, and a collisional gas using smoothed particle hydrodynamics.

In §2 we present straightforward analytical arguments. In §3 we describe the simulations setup, the codes used for analysis of the GADGET simulations, and present results for 3 different high resolution simulations with varying natal kick parameters for early black holes. In §4 we describe post-merger evolution through dynamical friction, before we conclude in §5.

2 ANALYTICAL EXPECTATIONS

Clustering of MBHs at the centers of dark matter halos leads to their growth into the population of IMBHs at the centers of merging dark matter halos. In the following sections we will address every dark matter halo that hosts a black hole as a parent halo. The early stages of the merger are driven by the hierarchical cold collapse of the sub-halos (gravitationally bound substructures of larger dark matter halos) into the primary halo (we focus our analysis on the single dark matter halo that naturally emerges from the numerical simulations as the largest in mass structure, hence the primary halo) forming the Galaxy. Subsequent dynamical evolution of the IMBH population occurs through dynamical friction, and secular orbital evolution in the presence of any residual triaxiality after virialization (Madau & Rees 2001, Holley-Bockelmann et al. 2001).

We assume that IMBHs embedded in their parent sub-halos experience dynamical friction acting collectively upon the entire compact sub-halo containing the IMBH, at least until tidal stripping significantly reduces the effective sub-halo mass to that of the central mass only (Weinberg 1989, Vine & Sigurdsson 1998). Tidal dissolution becomes effective only where the density of the primary halo is comparable to that of the sub-halo. With characteristic length scales of ~ 100 pc and masses of $\sim 10^6 M_\odot$, sub-halo densities are of order $10^{0\pm 1} M_\odot/pc^3$, and the primary halo density reaches such densities only in the inner few kpc, at radii $r \leq 0.01 r_{vir}$ (Fig 5).

The primary halo is well-approximated by a singular isothermal sphere for radii of order $0.1 r_{vir}$ (Madau & Rees 2001), the dispersion is near constant and isotropic over a range in radii, and the density profile is close to isothermal, with a steeper fall off at larger radii and flattening at smaller radii.

Approximating density interior to r , the distance of the sub-halo of mass M from the center of the primary halo, with associated circular velocity v_c to the center of the halo, timescale for dynamical friction to bring the sub-halo and associated IMBH to the primary halo center (Binney & Tremaine 1987, eq. 7.26) is:

$$t_{fric} = \frac{1.17 r^2 v_c}{\ln \Lambda GM}. \tag{1}$$

where $\ln \Lambda$ is Coulomb logarithm.

This is a conservative estimate for the time scale for early stages of dynamical friction; the orbits of the sub-halos are not circular and will therefore sink faster than we estimate, and coupling of the dynamical friction to internal degrees of the sub-halo also accelerates the evolution, possibly by as much as a factor of two (Weinberg 1989, Vine & Sigurdsson 1998). At small radii, mass loss from tidal disruption becomes significant, and the density profile flattens, but the dispersion also decreases, and we may expect the IMBH to continue their dynamical evolution towards the center of the primary halo, if they were close enough to get inside $r \leq 0.01 r_{vir}$ in the first place.

Typical mass ratios of early black holes and their host halos are $\geq 10^{-4}$. Consequently for kicks that expel the IMBH from their host-halos at the higher redshifts, the dynamical friction time scale is at least 10^4 times larger.

Assuming that dynamical friction is efficient in bringing sub-halo to the center of the primary halo, from the equation (1), we can calculate the radius r_{sink} at which sub-halo has to be, in order to sink to the center in less than the Hubble time for given velocity dispersion and sub-halo mass. If every sub-halo carries one IMBH at its center, then the merger rate for IMBHs will be function of number of sub-halos inside r_{sink} . If kicks at higher redshifts supply IMBH with enough velocity for IMBH to escape its sub-halo, the expected number of IMBHs at $r \leq r_{sink}$ will be smaller and this will lead to a significant decrease in IMBH merger rates. Stopping the growth of IMBH through gas accretion by ejecting them into lower dark matter density regions changes x-ray population predictions (Agol & Kamionkowski 2002). We illustrate these effects with N-body simulations in what follows.

3 ILLUSTRATIVE SIMULATION

3.1 Simulation Setup

We performed simulations that were set up for a cubic, periodic box of 14.3 comoving Mpc on a side in a Λ CDM universe with $\Omega_M=0.3$, $\Omega_\Lambda=0.7$ and $h=0.7$ from redshift $z=40$ to $z=1$. From initially low resolution simulations we selected a halo with $2 \times 10^{10} M_\odot$ at redshift one. We then refined a sphere of 2 Mpc comoving radius in the initial conditions and reran the simulations from $z=40$. Using 128^3 on the top level and a refinement factor of 4 in the high resolution region, we attain 4.9×10^6 high-resolution particles (softening length 2 kpc comoving) for the simulation and 2.0×10^6 low-resolution particles (softening length 4 kpc comoving) in the rest of the box. The mass of each high resolution particle in these simulations is $8.85 \times 10^5 M_\odot$ and the mass of each low-resolution particle is $5.66 \times 10^7 M_\odot$.

3.2 Analysis Tools

Every snapshot consists of masses, positions, and velocities of all types of particles at a specific redshift. Plots of their positions show clumps of particles that need to be associated with real-world objects. We used the HOP algorithm (Eisenstein & Hut 1998) to divide the particles into distinct sets such that particles in individual high-density regions are grouped together and left separate from those in other regions. HOP assigns density estimates to each particle by using the Gaussian smoothing algorithm and then determines, of the particle and its nearest neighbors, which of the particles has the highest density. Each particle is then associated with its highest density neighbor and hopping is continued to higher and higher densities until the highest density particle is reached. All particles that hop to the same maximum are placed into the same group. Every particle is assigned to one and only one group. To distinguish between the dense halo and its surroundings, we set a density threshold, cutting out of the group all particles with densities less than 5% of the density of the densest particle. We also define a halo as a group of more than 50 particles. The HOP output is a list of halos with IDs, coordinates, density of the densest particle, and number of particles in each halo. GADGET IDs of the particles are used for following the particles from one snapshot to another. They form different density distributions in different snapshots and applying HOP analysis will give us different densest particles in the same group in two different snapshots. HOP IDs are just following the order in which the particles are stored in the snapshot and they have to be matched with GADGET IDs if one wants to follow the dynamics of halos in the simulations.

Further analysis is performed by Ganyl, Gadget Analysis Code (Abel et al. 2001) and P-GroupFinder (Springel 2000). Ganyl analyzes spherical profiles for gadget data, taking both the list of centers from HOP analysis and a snapshot of the particle data that matches it. It converts units back to proper from comoving and brings particles into proper order according to their gadget IDs. Then, it identifies the centers in the snapshot, and goes in spheres from them to find the virial radii r_{200} , the total mass of the halos inside their virial radii m_{200} , theoretical velocity dispersion, components of angular momentum, and the total angular momentum. The virial radii are defined as radii enclosing mass density two hundred times of the mean mass density of the universe at the redshift of the snapshot.

P-GroupFinder is using a different approach for finding halos. Particle distribution is segmented into groups using the friends-of-friends (FOF) algorithm. Fraction of the mean interparticle separation is used as linking length and halos are defined with distance criteria only. Gravitationally self-bound substructures are then extracted from each FOF group by using SUBFIND algorithm. The bound part of FOF halo counts as subhalo as well, so every FOF halo has its bound counterpart.

These two different approaches in identifying halos are compared. Advantage of Ganyl is in its cosmological approach of defining halo using over-density, but since Ganyl is using density centers from the HOP algorithm, it is finding over-densities more than once for the same object creating artificial halos in this way. Since P-GroupFinder is checking for gravitational boundness, it can isolate one of these artificial halos as a real world object. Virial radii in kpc are calculated from total mass in particles ($100^{1/3} \times M_{tot}^{1/3}$) and their values are slightly larger than virial radii calculated by Ganyl. We use P-GroupFinder to identify black holes as the most bounded particles in their host halos.

We construct a merger tree from all 33 snapshots. The most massive halo incorporates hundreds of subhalos inside its virial radius. We examined all mergers and selected a sample of the most massive halos from each group of mergers together with a sample of isolated halos that do not merge. For this new list we found GADGET IDs of the centers of every halo and by tracing IDs in different snapshots, we identified coordinates and velocities to get trajectories of halo centers.

Density plots were made with codes provided by Naoki Yoshida which apply a spline SPH kernel to derived densities and then project them along one axis to produce a two dimensional smoothed image.

3.3 Black Holes Trajectories

The most massive halo in our simulation, at redshift $z=1$, (we will refer to this halo as primary from now on) has virial radius $R_{vir}=370$ kpc proper, and its mass inside this radius is $1.52 \times 10^{12} M_{\odot}$. We focused on studying properties of the primary halo and its substructure.

We assumed that at redshifts higher than $z=8$, every halo has an IMBH at its center. As Pop III remnants, formed before most other structure, IMBHs would have enough time to settle inside gravitational potentials of dark matter halos. From the simulation point of view this population can be selected by choosing every most-bounded particle in the halos discovered by P-GroupFinder. Tracking of this population through time can tell us how many IMBHs we can expect today inside galaxies and what their distribution would be. At redshift $z=8.16$ we identified 2869 dark matter halos with mass in range $10^7 M_{\odot} \lesssim M \lesssim 10^{10} M_{\odot}$. We selected the same number of IMBHs from their centers. By connecting particles' coordinates through 33 snapshots, we obtained MBHs trajectories from redshift $z=8.16$ to redshift $z=1.00$. From 2869 IMBHs at $z=8.16$, 1958 of them can be found inside primary halo at $z=1.00$. Fig 1. (top) shows density plot of XY-projection of SIM1 box at redshift $z=8.16$. Density peaks (in yellow) are the centers of dark matter halos selected by P-GroupFinder and in the same time the positions of particles which we selected for IMBHs. A sample of their trajectories (trajectories of IMBHs

from the hundred most massive halos) as they spiral inside the primary halo is overplotted. It is suggested (Miralda-Escude & Gould 2000) that clusters of IMBHs might exist inside the inner kpc of every galaxy, spiraling toward SMBH at the center.

3.4 Black Hole Kick Velocity

As mentioned in the introduction, coalescence under gravitational radiation may give an IMBH a significant kick velocity. We model the distribution of natal kicks with a truncated Gaussian in the interval $\{0, 150\}$ km s^{-1} , with a mean kick of 75 km s^{-1} . By an “IMBH” we are referring to the 2869 particles which define the centers of those sub-halos, at redshift 8.16, 3/4 of which are identified as destined to eventually merge with the primary halo. We add this presumed kick velocity with a random direction to a gadget velocity taken from the snapshot at redshift 8.16, for every particle identified as tracing the location of a presumed pop III IMBH. In this way, we obtain a new snapshot file with changed velocities of the group of black holes only. We use this snapshot file as an initial conditions file for a new simulation (SIM2a from now on) that starts at redshift 8.16, and we examine the differences in trajectories of the particles identified as tracers of the black holes, with and without natal kick velocities. The same procedure was repeated for different interval of velocities $\{125, 275\}$ km s^{-1} , with a mean kick of 200 km s^{-1} which was used for simulation - SIM2b. These are the most likely ranges suggested in the related works (Favata et al. 2004, Merritt et al. 2004).

Notice the fundamental difference between SIM1 and SIM2. In the case without the kicks, black holes embedded in sub-halos reach the center of the primary halo and the location of the presumed SMBH through dynamical friction. The main contribution to this process comes from the total mass of their halos which remain mostly bound through our simulation. In SIM2, IMBHs are generally ejected from their sub-halos by assigning new velocities and dynamical friction is not expected to be as efficient as in the first case since the dynamical friction mostly acts upon the bound sub-halo, not the much lower mass black hole (Hansen & Milosavljevic 2003, Gerhard 2001, Portegies Zwart 2003). Fig 1. (middle) and Fig 1. (bottom) show the density plot of XY-projection of SIM2a box (middle) and SIM2b box (bottom) at redshift $z=8.16$. As in SIM1, trajectories (from $z=8.16$ to $z=1$) of a sample of IMBHs are over-plotted. The same population of IMBHs, in three scenarios which differ only in IMBHs’ velocities, will have different trajectories depending on the kick assigned. In the first place, kicks have to be large enough to provide IMBHs with a velocity larger than the host halo escape velocity. If not, IMBH will not be able to escape the gravitational potential of the host halo and this will lead to a scenario quite similar to SIM1 (compare top and middle Fig 1.). Larger kicks, as in SIM2b, change IMBHs’ trajectories dramatically (compare top and bottom Fig 1.). Fig 2. explains the difference. Marked as pluses are the maximum escape velocities calculated from the gravitational potential of every dark matter halo selected at $z=8.16$. Escape velocity decreases with halo radius and reaches its maximum at the center. Hence, the maximum escape velocity is the escape velocity of IMBH since IMBH is the particle at the halo center. Escape velocity increases with the halo mass. Shown as circles are the velocities of IMBHs relative to their host halos at $z=8.16$ after assigning them kick centered at 75 km s^{-1} . The plot shows that IMBHs from less massive host halos have velocities larger than escape velocities. With the increase of host halo mass, IMBHs need to acquire larger velocities in order to escape from host halo gravitational potential and, for some of them, assigned kicks are not large enough (all the IMBHs that lie below data set are represented with pluses). These IMBHs continue the host halo original path toward primary halo as in the case of no kick. This process is demonstrated by the IMBHs in SIM2a (Fig 2. circles), hosted by most massive halos (kick velocities less than escape velocities). Since we plotted trajectories in Fig 1. only for IMBHs hosted by the hundred most massive halos, trajectories in Fig 1.-top and Fig 1.-middle are almost identical). This same set of IMBHs, but now with kick centered at 200 km s^{-1} in SIM2b (diamonds), almost all have enough velocity to escape host halos. As a result, trajectories in Fig 1.-top substantially differ from the trajectories in Fig 1.-bottom. Unlike Fig 1.-top and Fig 1.-middle, the IMBHs in Fig 1.-bottom leave their host halos at $z=8.16$ and as a result do not form binaries on their path to the primary.

Even though a substantial kick is assigned to black holes, and the dynamical friction does not play an important role for them anymore, they still manage to merge with the primary halo and some fraction of them makes way to the center to coalesce with the SMBH at the center of the halo. As the gravitational potential of dark matter halos increases at lower redshifts (Fig 3), kicked IMBHs are being captured and sink to the primary. Fig 3. shows maximum escape velocity as a function of dark matter halos’ mass at different redshifts for all halos identified in our simulation. The primary halo (thick line) goes through a large increase in gravitational potential toward lower redshifts. The maximum escape velocity from the primary halo increases from $\sim 250 \text{ km s}^{-1}$ at $z=8.16$ to $\sim 700 \text{ km s}^{-1}$ at $z=1$. Hence, the growth of the primary halo and the deepening of its gravitational potential well is responsible for the capture of IMBHs originally ejected from their host halos. However, the final spatial distribution of the presumed IMBHs is quite distinct (Fig 4), and their subsequent rate of coalescence with the central SMBH consequently may be different by orders of magnitude.

The number of IMBHs inside the primary halo at $z=1$ is 1958 and in SIM2a the number is only 14 IMBHs smaller. This is a coincidence, caused by the fact that we have changed velocities of all IMBHs identified at $z=8.16$ and not just of those that are being identified inside the primary halo at $z=1$. This means that some number of IMBHs that did not reach the primary halo originally, reached it in this new simulation because of the changed velocities and hence directions. Clearly the new IMBH arrive “naked”, without being enveloped in the dark matter sub-halos in which they formed originally. The number

of IMBHs inside the primary halo in both SIM1 and SIM2a originating from the same sub-halos, is 1851. Thus, 5.4% of the original population found in the primary halo, after change in their velocities at $z=8.16$, will not be found there. Similarly, a comparable number of the IMBHs that originally did reach the primary halo, will not in the repeated simulation.

Changes in trajectories of IMBHs in the repeated simulation with larger kicks (SIM2b) is more pronounced (Fig 1. bottom). With larger kicks, more IMBHs attain velocities large enough to leave their host halos. Although they need more time to sink into the potential well of the primary halo, 1795 of them reach the primary halo at redshift $z=1$. The number of IMBHs originating from the same sub-halos as in SIM1 is 1630. Thus, 16.7% of the original population is lost due to the kicks, but for the same reason, a new population of IMBHs is kicked into the primary halo, which in total gives 1795 IMBH - meaning that the primary halo in SIM2b will have only 8.3% of IMBHs less than the primary halo in SIM1.

4 POST-MERGER EVOLUTION

We find that significantly more black holes get at the center of the primary halo when they are embedded in their dark matter sub-halos. But a number of mergers to the center occur even in the presence of kicks. Fig 4. shows the number density of the IMBHs inside the primary halo, from SIM1, SIM2a and SIM2b. Although the total number of black holes differs from SIM1 by 0.7% for SIM2a and 8.3% for SIM2b, there is a decrease in the number of IMBHs at SIM2 for the inner 10% of the primary halo.

We now estimate the dynamical friction time scale for the IMBH and sub-halo sinking in the gravitational potential of the halo. From eqn 1), for the singular isothermal sphere with circular velocity v_c , the velocity dispersion is $\sigma=v_c/\sqrt{2}$, the virial radius of the halo is $r=r_{vir}$, and the mass inside this radius is $1.52\times 10^{12} M_\odot$. For the primary halo these values are $r_{vir}=370\text{kpc}$ comoving, velocity dispersion $\sigma = 157 \text{ km s}^{-1}$, and impact parameter $b_{max}=r_{vir}$. We calculate a radius (r_{sink}) which IMBHs have to reach in order to merge to the center in less than the Hubble time. We distinguish two cases. First, when the IMBHs are inside sub-halos of minimum mass $10^7 M_\odot$ (SIM1). Second, when IMBH has been ejected from its parent sub-halo (SIM2). In the first case, IMBH is brought to some radius inside the primary halo by the parent sub-halo and will continue sinking toward the center embedded within it. If we plug in Hubble time in formula (1), for the above values of velocity dispersion and mass we calculate that due to dynamical friction IMBHs inside $10^7 M_\odot$ will merge to the center if they are at less then $r_{sink}=r_{vir}/30$ when the halo collapse virialises. We find that a little over 4% of the IMBHs formed are at radii less then r_{sink} . So for this model we predict that in the absence of kick, 83 IMBH reach the center to coalesce with the central SMBH (or the seed SMBH formed in the sub-halo that became the center of the primary halo). More generally, this predicts $O(10^2)$ IMBH mergers per Milky Way like halo over a Hubble time, even for the cases shown here where only halos with masses $\geq 2.83 \times 10^7$ were allowed to form black holes. Since there are $\sim 10^{10}$ galaxies in the observable universe in this mass range, the LISA' merger rates will be $\sim 10^{12}$ per Hubble time or $R\sim 100/\text{year}$.

In the second case, the kicked IMBHs have a significantly flatter spatial distribution, partly because they have decoupled from their parent sub-halos, so there are fewer inside $1/30r_{vir}$. Fig 4. shows that there are 2.21% of IMBHs from SIM2a and 0.95% of IMBHs from SIM2b inside this radius. Fig 5. shows the ratio of IMBHs with kicks and IMBHs with no kicks. There is a large drop in the central population of IMBHs with kicks. This can be seen also in density plots Fig 6. By repeating the same calculation as in the previous case with the only difference in the value for mass in the equation for dynamical friction, $8.85\times 10^5 M_\odot$ instead of $10^7 M_\odot$, (notice that we use particles as tracers of IMBH, in reality IMBH has smaller mass and needs to get to smaller radii for dynamical friction to be efficient) since that is the mass of single particle, we calculate that in order to merge at the center, IMBHs in SIM2 have to be at radii less then $r_{sink}=r_{vir}/100$. Only 1/4% of the SIM2a IMBHs are inside this radius. That is, under the same assumptions but allowing for natal kicks, only about 4 to 5 IMBH merge with the central SMBH over Hubble time, a factor of 20 lower merger rate. In the SIM2b there are no IMBHs inside $r_{vir}/100$ except for the one originating from the ancestor of primary halo at redshift $z=8.16$. These numbers can increase since, in reality, σ is lower at small radii so t_{fric} is also smaller. The merger of 83 IMBHs in SIM1 leads to formation of $7\times 10^7 M_\odot$ SMBH inside the dark matter halo with velocity dispersion $\sigma = 157 \text{ km s}^{-1}$. From the cosmological Monte Carlo realizations of the merger hierarchy (Volonteri et al. 2003), SMBH of the same mass and halo velocity dispersion would be formed only when mergers are combined with gas accretion as mechanisms for SMBH formation. Both results are below empirical values (Ferrarese et al. 2002). We note that the primary halo is not actually spherical and if a halo is triaxial, then some fraction of the IMBHs can “walk” into the inner halo ($r \ll 10^{-2}r_{vir}$) region on time scale $\sim 10t_{orbital}$ due to centrophilic box or boxlet orbits (de Zeeuw 1985, Zhao et al 2002, Holley-Bockelmann et al. 2005), at which point dynamical friction becomes effective in bringing the IMBH to the halo center. Also, some of the IMBHs are being assigned with kick velocities that directed them toward center. Due to this, some additional IMBHs from SIM1 and SIM2 could reach orbits in the center of HALO 1. We will explore the consequences of the non-spherical shape of the primary halo on the long term dynamical evolution of the sub-halos, and the implications for black hole mergers and evolution of the inner regions of the galaxy in another paper (in preparation).

Kicks are also responsible for ejecting IMBHs from the gas enriched regions of the halos. Since gas accretion is one of the main mechanisms for black hole growth, dumping black holes into regions of lower gas densities would prevent formation of

AGNs which would lead to a decrease in their numbers. Gas accumulates where the gravitational potential wells are deepest. It is also where dark matter densities are highest. Therefore we may get a crude estimate of the ability of IMBHs to accrete gas by tracing the dark matter density at their positions. Fig 7. shows average local density of dark matter traced by our set of IMBHs vs. redshifts. At $z=8.16$ the kicks are assigned. IMBHs are being ejected from their host halos into the regions with lower density (dash and dash-dot from $z=8.16$ to $z=7.75$). From $z=7.75$ to $z=2.80$ kicked IMBHs are in the environment 1-6 times less dense than in the no-kick case. This might suppress formation of AGNs. Notice that around $z=3.00$, the average IMBHs in all three cases start tracing similar density distributions. This implies that for $z \geq 3$, the contribution of faint AGNs to the ionizing background would be decreased if kicks of IMBHs were important.

5 DISCUSSION

We have performed and analyzed high-resolution collisionless simulations of the evolution of structure in a Λ CDM model. We have followed the formation and evolution of dark matter halos and by assuming that each halo is a host of one IMBH we have studied the formation of SMBH. We focused on two specific cases. First, IMBHs together with their host halos merge through dynamical friction. Second, when IMBHs are endowed with an initial kick, this leads to the ejection from their host halos in many cases. Analytically it is clear that the dynamical friction will act more efficiently on the host halos than on the much lower mass black holes formed within them. Our illustrative calculations highlight some of the expected differences in the density distribution of the final distributions of black holes which may be quite different, even in the presence of the modest kick velocities we have imposed.

In order for dynamical friction to work in numerical simulations, the density of the background - primary halo density - has to be more resolved. Larger resolution gives smaller softening lengths for particles and smaller softening lengths give more realistic dynamical friction. At the current resolution of our simulation, dynamical friction can not be efficiently realized in the model after $z \sim 1$ and $r \lesssim r_{vir}/30$ because the background density of parent halos is not resolved well enough. Even at the current resolution, our simulations are able to account for effects of dynamical friction on the sub-halos at high z . Subsequent papers will track the dynamical evolution of the sub-halos and IMBH at late times, using higher resolution simulations and semi-analytic implementations of dynamical friction (Binney & Tremaine 1987). A little over 4% of IMBHs merge at the center in less than Hubble time. If this is the dominant way of creating SMBH then it is efficient even if the IMBHs are ejected from their parent halos, with merger numbers only reduced by a factor of two or so for modest kicks. It is also possible that kick velocities have been underestimated in our simulations. The value of the median kick of 150km/s may be increased to more than 1000km/s according to some authors (Favata et al. 2004, Merritt et al. 2004) which would also greatly enhance the effects introduced here, reducing the number of mergers too negligibly small. LISA observations should strongly constrain any natal kick on IMBHs formed from very massive Pop III stars in low mass proto-galactic sub-halos.

REFERENCES

- Abel, T., Bryan, G., & Norman, M., 2000, ApJ, 540, 39
 Abel, T., Bryan, G., & Norman, M., 2002, Sci, 295, 93A
 Agol, E. & Kamionkowski, M., 2002, MNRAS, 334, 553
 Agol, E., Kamionkowski, M., Koopmans, L. V. E., & Blandford, R. D., 2002, ApJL, 576, L131
 Arzoumanian, Z., & Cordes, J. M., Chernoff, D., 1997, AAS, 19111308A
 Binney, J., & Tremaine, S., 1987, Galactic Dynamics (Princeton: Princeton Univ. Press)
 Brandt, S. & Anninos, P., 1999, PhRvD, 60h4005B
 Brandt, W. N., Podsiadlowski, Ph., & Sigurdsson, S., 1995, MNRAS, 277L, 35B
 Bromm, V., Coppi, P. S., & Larson, R. B., 2002, ApJ, 564, 23
 Colpi, M., & Wasserman, I., 2002, ApJ, 581, 1271
 Couchman, H. M. P. & Rees, M. J., 1986, MNRAS, 221, 53
 Cornish, N. J., & Levin, J., 2002, gr-qc/0207016
 Danzmann, K., 2003, AdSpR, 32, 1233D
 Davies, M. B. et al. 2002, ApJ, 579L, 63
 Eisenstein, D., & Hut, P., 1998, ApJ, 498, 137
 Miralda-Escude G., & Gould A., 2000, 545, 847M
 Favata M., Hughes S. A., & Holz D. E., 2004, ApJL, 607, L5
 Ferrarese L., 2002, ApJ, 578, 90
 Gebhardt, K. et al. 2001. & ApJ, 555L, 75G
 Gerhard, O., 2001, ApJL, 546L, 39G
 Graham, A. W., et al. 2001, ApJ, 563, L11
 Hansen, B.M.S., & Milosavljevic, M., ApJL, submitted, astro-ph/0306074
 Heger et al., 2003, 2003, ApJ, 591, 288H
 Holley-Bockelmann, K., & Mihos, J.C., Sigurdsson, S., Hernquist, L., 2001, ApJ, 549, 862
 Holley-Bockelmann, K., & Mihos, J.C., Sigurdsson, S., Hernquist, L., Norman, C., 2002, ApJ, 567, 817

- Holley-Bockelmann, K., & et al. 2005, DDA, 36.0206H
Islam, R. R., Taylor, J. E., Silk, J., & 2003, MNRAS, 340, 647I
Lai, D., Chernoff, D.F., & Cordes, J.M., 2001, ApJ, 549, 1111
Laor, A., 2001, ApJ, 553, 667
Kormendy, J., & Gebhardt K., 2001, XX Texas Symposium on Relativistic Astrophysics, & New York: Am. Inst. Phys., p 363
Madau, P., & Quataert, E., 2004, astro-ph/0403295
Madau, P., Rees M. J., 2001, ApJ, 551L, 27M
Mao, S. & Paczyński, B., 2002, MNRAS, 337, 895
Merritt, D., & Ferrarese, L., 2001, MNRAS, 320, L30
Merritt, D., Milosavljevic M., & Favata M., Hughes S. A., Holz D. E., 2004, ApJ, 607, L9
Micic, M., Abel, T., & Sigurdsson, S., 2004, proceedings of 22nd Texas Symposium on Relativistic & Astrophysics at Stanford University.
Portegies Zwart, S.F., McMillan, S., & Gerhard, O., 2003, ApJ, submitted, astro-ph/0303599
Redmount, I. H. & Rees, M. J. 1989, Comments on Astrophysics, 14, 165
Rees, M., J., 1988, Nature, 333, 523R
Schneider, R., Ferrara, A., & Natarajan, P., Omukai, K., 2002, ApJ, 571, 30
Springel, V., Yoshida, N., & White, S. D. M., 2001, NewA, 6, 79
Springel, V., 2000, MPA
Thorne, K., 1995, NYASA, 759, 127
Tremaine, S., Gebhardt, K., & Bender, R., 2002, ApJ, 574, 740T
Valtonen, M., Mikkola, S., & Heinamaki, P., 2000, sgg, conf, 310V
Vecchio, A., Wickham, E. D., Stevens, I. R., & 2004, SPIE, 5500, 183V
Vine, S., Sigurdsson, S., & 1998, MNRAS, 295, 475
Volonteri, M., Haardt, F., & Madau, P., 2003, ApJ, 582, 559
Weinberg, M., 1989, ApJ, 239, 549
Wex, N., Kalogera, V., & Kramer, M., 2000, ApJ, 528, 401
Xu, G., 1994, ApJ, 437, 184X
de Zeeuw, T., 1985, MNRAS, 216, 273
Zhao, H-S., Haehnelt, H.G., & Rees, M.J., 2002, NewAst., 7, 385

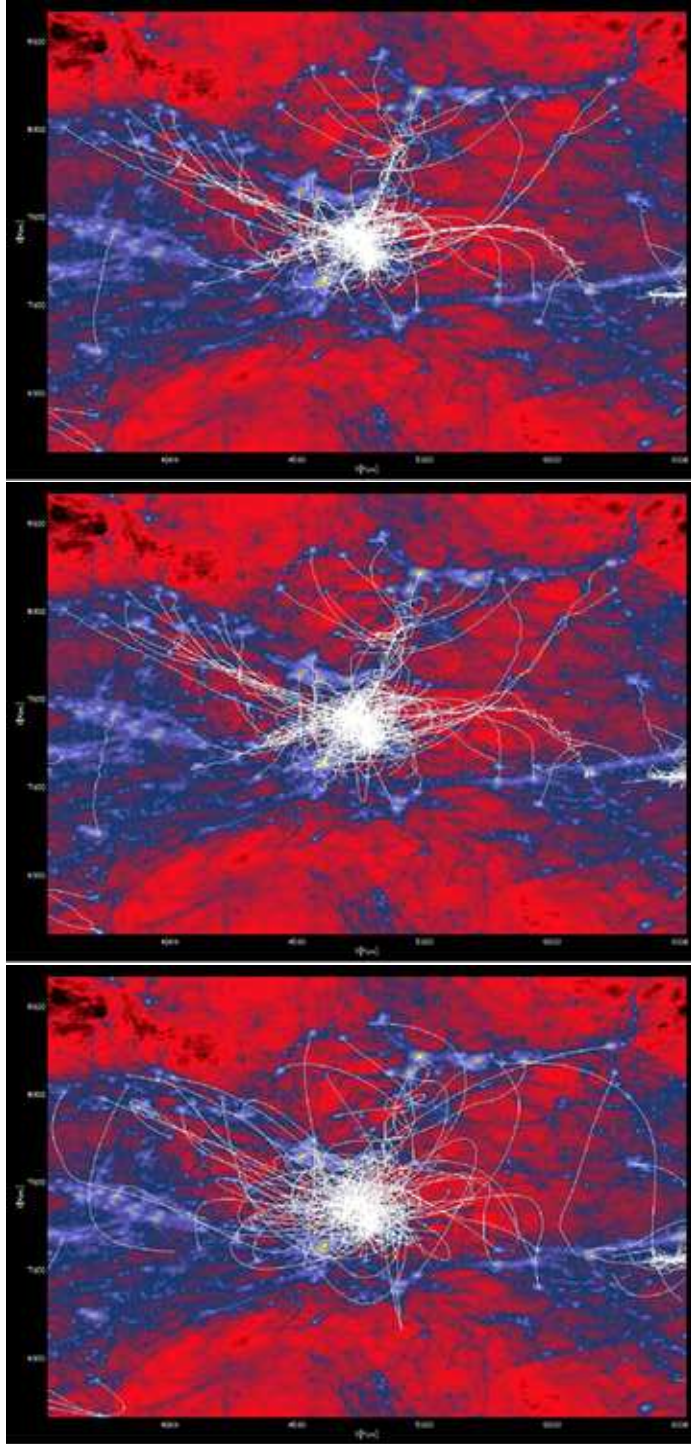


Figure 1. Sample of hundred IMBHs selected from most massive host halos at $z=8.16$ and their trajectories (white) from $z=8.16$ to $z=1$ overlotted on 2D density projection. Density peaks in yellow correspond to host halos centers at $z=8.16$ and to the positions of their IMBHs. top: no kick case (SIM1); middle (SIM2a): case of $[0,150]$ km/s kick centered at 75km/s and bottom (SIM2b): case of $[125,275]$ km/s kick centered at 200km/s. With large kicks IMBHs overcome the host halos gravitational potential resulting in change of their trajectories and the final distribution of IMBHs (smearing of the trajectories at the center, quantified in the later plots). Observe, e.g., the upper right corner of all tree plots where two IMBHs form a binary in SIM1 and SiM2a. In SIM2a, IMBHs are trying to escape but the gravitational potential of dark matter halos is pulling them back. In SIM2b, assigned kick is larger than in SIM2a and also large enough to prevent formation of binary. Underneath this binary in SIM1, at the coordinates $[5700,7000]$ kpc, a dense halo center hosts an IMBHs. In less than 100kpc, this halo captures three IMBHs more. This small “cluster” of IMBHs spirals in toward the center. The picture clearly resolves IMBHs orbits around center of mass up to the point, $[5200,7400]$ kpc, where the orbital separation is smaller than the softening length. This point is reached later in SIM2a because of the kicks while in SIM2b binaries never form.

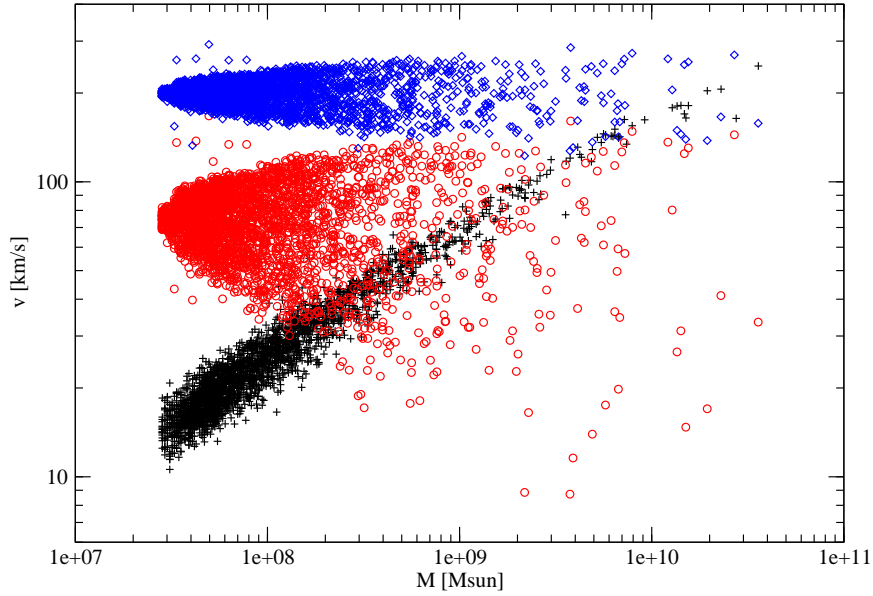


Figure 2. Black holes' escape velocity as a function of halo mass ($z=8.16$) as pluses, calculated from gravitational potential of host halo set consisting of 2869 members. Black holes' velocity relative to their host halos' velocity reduce to assigned kicks: $[0,150]$ km/s centered at 75 km/s represented as circles and $[125,275]$ km/s centered at 200 km/s represented as diamonds. Lower mass host halos have lower maximum escape velocities enabling their IMBHs to escape. IMBHs in more massive host halos demand larger kicks in order to escape. As a result, some of them stay captured in their host halo gravitational potential.

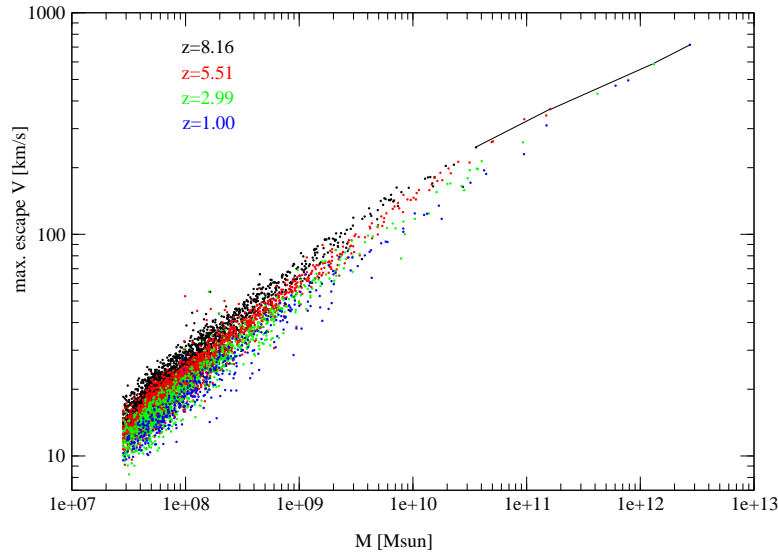


Figure 3. Maximum escape velocity (corresponds to central gravitational potential) of dark matter halos at different redshifts as a function of dark matter halos' masses. Gravitational potential of the primary halo (thick line) increases at lower redshifts capturing even the IMBHs which have been assigned with the highest kick velocities.

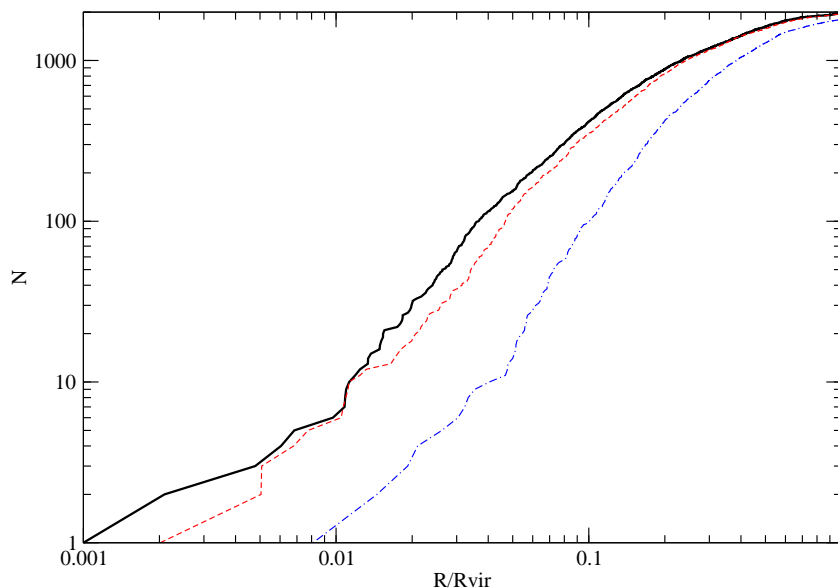


Figure 4. Number of black holes as a function of primary halo radius. No kick case (thick); $[0,150]$ km/s kick centered at 75 km/s (dash) and $[125,275]$ km/s kick centered at 200 km/s (dash-dot). Although the number of IMBHs entering primary halo is comparable in all three cases, the difference in their interior distribution is well pronounced.

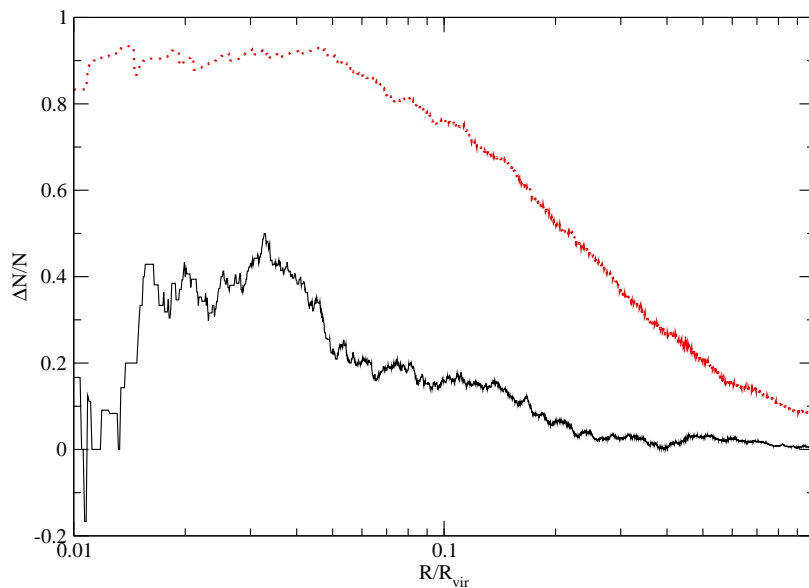


Figure 5. Fraction of SIM1 black holes in SIM2a and SIM2b as a function of radius. thick line for $[0,150]$ km/s kicks centered at 75 km/s and dots for $[125,275]$ km/s kicks centered at 200 km/s.

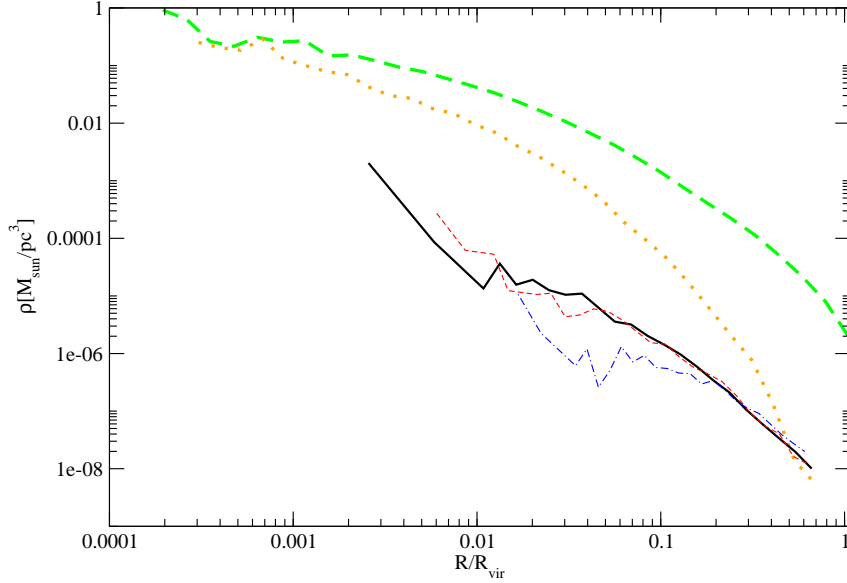


Figure 6. Density of the primary halo at $z=1$ (thick dash) and its most massive progenitor from $z=8.16$ (dots) as a function of radius. Also, density in hosted black holes for no kick (thick); $[0,150]$ km/s kick centered at 75 km/s (dash) and $[125,275]$ km/s kick centered at 200 km/s (dash-dot).

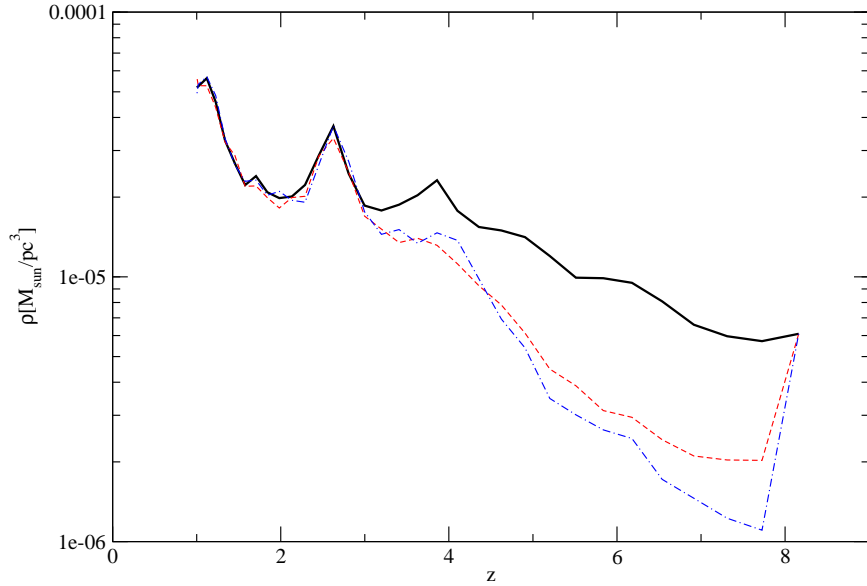


Figure 7. Local density of dark matter traced by black holes as a function of redshift. No kick (thick); $[0,150]$ km/s kick centered at 75 km/s (dash) and $[125,275]$ km/s kick centered at 200 km/s (dash-dot). Ejection of IMBHs from gas enriched regions of galaxy influences AGNs formation rates, reduces their numbers and their contribution to ionizing background.